

ENSO flavors in a tree-ring $\delta^{18}\text{O}$ record of *Tectona grandis* from Indonesia

Karina Schollaen^{1,2}, Christina Karamperidou³, Paul Krusic^{4,5}, Edward Cook⁶,
Gerhard Helle¹

[1] (GFZ - German Research Centre for Geosciences, Section 5.2 Climate Dynamics and Landscape Evolution, Potsdam, Germany)

[2] (Alfred Wegener Institute Helmholtz Centre for Polar and Marine Research, Potsdam, Germany)

[3] (Department of Meteorology, University of Hawai'i at Manoa, Honolulu, Hawai'i, USA)

[4] (Navarino Environmental Obs. Messinia, Greece)

[5] (Department of Physical Geography and Quaternary Geology, Stockholm University, Stockholm, Sweden)

[6] (Tree Ring Laboratory, Lamont-Doherty Earth Observatory, Columbia University, USA)

Correspondence to: K. Schollaen (karina.schollaen@gmail.com)

Abstract

Indonesia's climate is dominated by the equatorial monsoon system, and has been linked to El Niño-Southern Oscillation (ENSO) events that often result in extensive droughts and floods over the Indonesian archipelago. In this study we investigate ENSO-related signals in a tree-ring $\delta^{18}\text{O}$ record (1900-2007) of Javanese teak. Our results reveal a clear influence of Warm Pool (central Pacific) El Niño events on Javanese tree-ring $\delta^{18}\text{O}$, and no clear signal of Cold Tongue (eastern Pacific) El Niño events. These results are consistent with the distinct impacts of the two ENSO flavors on Javanese precipitation, and illustrate the importance of considering ENSO flavors when interpreting palaeoclimate proxy records in the tropics, as well as the potential of palaeoclimate proxy records from appropriately selected tropical regions for reconstructing past variability of ENSO flavors.

1 Introduction

The tropical warm pool surrounding the Indonesian maritime continent (IMC) is a region of homogenous sea surface temperatures where atmospheric deep convection occurs, and plays a key role in the regulation of the global tropical climate (Clement et al., 2005; Pierrehumbert, 1995).

1 Indonesia's regional climate is governed by the Australian-Indonesian Monsoon (Wheeler and
2 McBride, 2005) and the associated seasonal movement of the Inter Tropical Convergence
3 Zone (ITCZ). Variations of the equatorial monsoon system significantly impact the livelihood
4 of over 230 million people living in the world's fourth most populated country.

5 The El Niño-Southern Oscillation (ENSO) phenomenon contributes to the rainfall pattern of
6 the IMC and has been thought to interact with the monsoons (e.g. Hendon, 2003; Lau and
7 Nath, 2000). Recent studies have drawn attention to the existence of more than one variant or
8 '*flavors*' of El Niño (the warm phase of ENSO) (Ashok et al., 2007; Kug et al., 2009; Larkin
9 and Harrison, 2005; Ren and Jin, 2011; Takahashi et al., 2011). The canonical El Niño
10 (Sarachik and Cane, 2010), also referred to as eastern Pacific (EP) El Niño (Kao and Yu,
11 2009) or Cold Tongue El Niño (Kug et al., 2009; Ren and Jin, 2011), exhibits SST anomalies
12 localized in the eastern equatorial Pacific. The El Niño variant with maximum SST anomalies
13 located in the central equatorial Pacific is referred to as the central Pacific (CP) El Niño (Kao
14 and Yu, 2009), Warm Pool (WP) El Niño (Kug et al., 2009; Ren and Jin, 2011), date line El
15 Niño (Larkin and Harrison, 2005) or El Niño Modoki (Ashok et al., 2007; Takahashi et al.,
16 2011). In this study we use the terms Cold Tongue (CT), and Warm Pool (WP) El Niño (Ren
17 and Jin, 2011) to describe these two ENSO flavors.

18 Identifying the mechanisms responsible for the CT and WP ENSO flavors is an active field of
19 research. At present, there is no consensus on whether a reported increase in the frequency
20 and intensity of WP ENSO events in recent decades (Ashok et al., 2007; Kao and Yu, 2009;
21 Kug et al., 2009; Lee and McPhaden, 2010) is a result of anthropogenic greenhouse gas
22 forcing (Yeh et al., 2009), or natural variability (McPhaden et al., 2011; Newman et al.,
23 2011). In addition, the simulation of ENSO flavors in Global Climate Models (GCMs) is still
24 subject to limitations in our understanding of the phenomenon. Consequently, there is much
25 uncertainty about whether ENSO activity will be enhanced or damped in the future, or if the
26 relative frequency of ENSO flavors will change (Collins et al., 2010). Long records of ENSO
27 activity are essential for identifying trends and multidecadal changes in the patterns of sea
28 surface temperature associated with ENSO, making palaeoclimate reconstructions particularly
29 attractive for shedding light onto the past and future of ENSO flavors.

30 Recent research on ENSO-proxy teleconnections recommends, that when interpreting proxy
31 data, differences in the influence of the two ENSO flavors on SST, precipitation and salinity
32 should be taken into account (Karamperidou et al., 2015). Certain regions like Java lie in key
33 locations where interannual precipitation variability is significantly correlated to one ENSO
34 flavor but not the other (see Fig. 1). Thus, long-term rainfall proxies from Java can be useful

1 for distinguishing between ENSO flavors, and for studying their relation to monsoon
2 variability.

3 Over the last decade there have been several attempts to reconstruct continuous time series of
4 ENSO variability using different proxy archives such as corals (e.g. Abram et al., 2008;
5 Charles et al., 2003; Cobb et al., 2013; Evans et al., 2002; Linsley et al., 2004; Pfeiffer et al.,
6 2009; Quinn et al., 2006; Wilson et al., 2006), tree-ring widths (e.g. D'Arrigo et al., 2005;
7 Fowler et al., 2012; Stahle et al., 1998) or tree-ring stable isotopes (Sano et al., 2012).
8 Furthermore, several multi-proxy reconstructions of ENSO variability are available (e.g.
9 Braganza et al., 2009; D'Arrigo et al., 2006; Emile-Geay et al., 2013; Mann et al., 2000;
10 Wilson et al., 2010). However, many of these reconstructions are based on extratropical proxy
11 records, particularly from tree-ring widths, and thus do not represent ENSO activity directly.

12 Tree-ring stable isotopes often provide additional climate information where the more
13 commonly used tree-ring proxies (e.g., ring width and maximum latewood density) do not, or
14 where the teleconnection signal is weak. In tropical regions, oxygen isotope data from tree
15 rings ($\delta^{18}\text{O}_{\text{TR}}$) are often more sensitive to precipitation than ring width (e.g. Brien et al.,
16 2012; Scholten et al., 2013). $\delta^{18}\text{O}_{\text{TR}}$ data are primarily controlled by the isotopic composition
17 of precipitation, i.e. the source water, and relative humidity (e.g. Barbour, 2007; McCarroll
18 and Loader, 2004). The isotopic composition of precipitation ($\delta^{18}\text{O}_{\text{Pre}}$) depends on a number
19 of factors, the so-called 'kinetic isotope effects' (Araguás-Araguás et al., 2000). One of these
20 effects, 'the amount effect', is the inverse correlation between rainfall amount and $\delta^{18}\text{O}_{\text{Pre}}$
21 values, and a crucial driver in determining $\delta^{18}\text{O}_{\text{Pre}}$ values in the tropics (e.g. Brien et al.,
22 2012; Zhu et al., 2012). Thus $\delta^{18}\text{O}_{\text{TR}}$ records offer a promising approach to examine monsoon
23 activity, and large-scale climate variations such as ENSO.

24 In previous studies we investigated relationships between seasonal rainfall variability and
25 tree-ring stable isotope records from Javanese teak trees on inter- to intra-annual time scales
26 (Scholten et al., 2014; Scholten et al., 2013). In this study we explore the signal strength of
27 ENSO flavors in our annually resolved $\delta^{18}\text{O}_{\text{TR}}$ record from Java, the only well replicated,
28 centennial $\delta^{18}\text{O}$ record from Javanese teak in existence. We place particular emphasis on the
29 time stability of the teleconnected $\delta^{18}\text{O}$ /ENSO relationship. To the best of our knowledge this
30 is the first time the relationship between tree-ring proxies and the two ENSO flavors has been
31 tested. We find a unique WP El Niño signal in the $\delta^{18}\text{O}_{\text{TR}}$ record from Java, supporting the
32 notion that proxies from carefully selected regions are valuable for answering questions of
33 past and present ENSO variability, and for constructing reliable ENSO reconstructions.

2 Data and Methods

2.1 Proxy data and site description

We use a tree-ring $\delta^{18}\text{O}$ chronology from a lowland rainforest in the eastern part of Central Java, Indonesia (07°52'S, 111°11'E; 380 m a.s.l.), spanning the period 1900-2007. The $\delta^{18}\text{O}_{\text{TR}}$ record is built from resin-extracted wood of 7 teak (*Tectona grandis*) trees, collected from the Donoloyo Cagar Alam (site DNLY in D'Arrigo et al., 2006) shown as green lines in Fig. 2. The according TRW chronology dates back to AD 1714. This $\delta^{18}\text{O}_{\text{TR}}$ chronology and its dendroclimatological potential as a rainfall indicator has been described in detail in Schollaen et al. (2013). Indonesia receives significant rainfall year-round but experiences a distinct wet and dry season. The wet season (approx. October/November to April/May) coincides with movement of the Inter-Tropical Convergence Zone to the Southern Hemisphere, while the dry season (June to September) corresponds with a predominance of dry southeasterly winds from Australia (Aldrian et al., 2007). The isotopic composition of precipitation ($\delta^{18}\text{O}_{\text{Pre}}$) over Java shows that distinct seasonal changes are linked to rainfall amount resulting in high $\delta^{18}\text{O}_{\text{Pre}}$ values during the dry season, and low $\delta^{18}\text{O}_{\text{Pre}}$ values during the rainy season (Fig. 5b, Schollaen et al., 2014). Instrumental records (e.g. Aldrian and Susanto, 2003; Allan, 2000; Haylock and McBride, 2001) and reanalysis products (Aldrian et al., 2007; Jourdain et al., 2013) show rainfall anomalies in Indonesia are affected by ENSO: During a warm ENSO phase (El Niño events) the tropospheric air flow (Walker Circulation) weakens and the Indonesian Low pressure system migrates eastward into the tropical Pacific, resulting in drought over much of the country. Conversely, a cold ENSO phase (La Niña events) brings excess rain to the region (Sarachik and Cane, 2010). Several analyses of Indonesian rain gauge data show that Indonesian rainfall is poorly correlated with ENSO events during the wet monsoon season, but reveal highest coherence during the dry season and transition months prior to the wet season (June to November) (Haylock and McBride, 2001; Hendon, 2003). However, taking the IMC and surrounding oceanic rainfall into account, rainfall during the wet season is also related to ENSO (Fig. 8a, Jourdain et al., 2013).

In this study, we further show that precipitation anomalies in Java are sensitive to ENSO flavors. Fig. 1 shows the relationship between precipitation data and the WP and CT ENSO indices (see Sect. 2.2 for definition of the indices) for the IMC and Pacific region. WP El Niños are associated with drought over Java (Fig. 1, upper panel), and have a strong influence on the Australian-Indonesian monsoon system (e.g. Kumar et al., 2006; Taschetto and England, 2009). On the other hand, Java lies on the nodal line of influence of CT El Niños (Fig. 1, lower panel), which makes it a key location for obtaining records able to distinguish

between the two ENSO flavors. The average regression coefficient between monthly precipitation anomalies over Java and the WP ENSO index is -0.83 mm/day, while for CT ENSO it is -0.03 mm/day (non-significant).

The growing season for teak in Central and Eastern Java occurs mostly during the wet season, from October to May (Coster, 1928, 1927; Geiger, 1915; Schollaen et al., 2013). In all subsequent analysis, we use the southern hemisphere convention, which assigns to each tree ring the year in which radial growth begins (Schulman, 1956). Thus lag-0 refers to the year n where tree growth starts: Oct _{n} -Sep _{$n+1$} . Lag-1 refers to Oct _{$n-1$} -Sep _{n} .

2.2 Definition of ENSO flavors

In the following, we use the global SST dataset of Kaplan et al. (1998). To calculate indices for the two ENSO flavors we use the coordinate transform of the NINO3-NINO4 phase space proposed by Ren and Jin (2011) and shown in Equation 1.

$$\begin{aligned} N_{CT} &= N_3 - \alpha N_4 \\ N_{WP} &= N_4 - \alpha N_3, \end{aligned} \quad \alpha = \begin{cases} 2/5 & \text{if } N_3 \cdot N_4 > 0 \\ 0 & \text{otherwise} \end{cases} \quad (1)$$

where N_{CT} , N_{WP} are the indices for CT and WP ENSO, and N_3 , N_4 are the NINO3 and NINO4 indices, i.e. the SST anomaly averaged over the regions [5N-5S, 150W-90W] and [5N-5S, 160E-150W] respectively. The timeseries of the two indices N_{CT} , N_{WP} are shown in Figure 2a and b (January values). When a Warm Pool event occurs (e.g. 1994-95), SST anomalies are mostly concentrated in the NINO4 region, and therefore the N_{CT} index resulting from Equation 1 is very small. In contrast, the N_{WP} index, which is dominated by the NINO4 anomalies, is large and, thus, the event is classified as a Warm Pool event. The opposite occurs during large Cold Tongue events (e.g. 1976-77, 1982-83, and 1997-98): NINO3 anomalies dominate NINO4, and thus the N_{WP} index is very small compared to N_{CT} , and the event is classified by Equation 1 as a Cold Tongue event. As shown in detail in Ren and Jin (2011), the two indices are able to capture the SST anomaly patterns that characterize the two ENSO flavors, as well as their variability in the 20th century. No significant differences were found when using alternative indices (Ashok et al., 2007; Takahashi et al., 2011) for calculating ENSO flavors (not shown here). Distinguishing between the two corresponding types of La Niña events, as advocated by Kao and Yu (2009) and Ashok and Yamagata (2009), may not be necessary because the SST and precipitation patterns of the two La Niña types are not very distinctive (Kug and Ham, 2011) and the SST anomalies during La Niña events generally tend to propagate westward. Therefore a single index (NINO4) suffices to

capture La Niña events, as shown in Figure 2c, and a coordinate transform of two indices (as in equation 1 above) is not necessary.

For subsequent analyses we use the January (Jan_{n+1}) indices for the ENSO flavors, for the timespan 1900–2007. We focus on the month January as that represents the month with highest precipitation during the rainy season at the study site. Here, our $\delta^{18}\text{O}_{\text{TR}}$ record correlates the best with regional rainfall data (Schollaen et al., 2013). We classify each year as CT, or WP when N_{CT} , or N_{WP} are greater than one standard deviation of the respective monthly index. We classify a year as La Niña (LN) when NINO4 is negative by less than one standard deviation of the monthly NINO4 index. Table 1 shows the list of years classified as CT, WP, and LN according to the above criteria.

2.3 ENSO signal assessment

To assess the long-term temporal stability of the ENSO signal, running 31-year correlations were calculated between the $\delta^{18}\text{O}_{\text{TR}}$ record and the varying ENSO flavors. A Kalman filter analysis was also used as a time-dependent regression-modeling tool to test the temporal stability of the relationship between the $\delta^{18}\text{O}_{\text{TR}}$ record and the two ENSO flavors. In contrast to the running correlation procedure, the Kalman filter method uses maximum likelihood estimation to objectively test for the identification of time-dependence between predictor and predicted variables (see Visser and Molenaar (1988) for details, and Cook et al. (2002), Cook et al. (2013) or Wilson et al. (2013) for examples).

Furthermore, probability density functions of the correlation between $\delta^{18}\text{O}_{\text{TR}}$ variability and the different ENSO phases (WP, CT and LN), as well as during neutral conditions, were calculated. We classify neutral conditions when CT or WP are not greater than one standard deviation of the respective monthly index and when LN is negative by more than one standard deviation of the monthly NINO4 index. Finally, the spectral properties of the $\delta^{18}\text{O}_{\text{TR}}$ proxy time series were analyzed (Schulz and Mudelsee, 2002) and wavelet coherency analysis performed (Grinsted et al., 2004; Torrence and Compo, 1998).

3 Results

Monthly and seasonal correlations between the Javanese $\delta^{18}\text{O}_{\text{TR}}$ record (Fig. 2, green line in all plots) and ENSO flavors (see section 2.2) were computed for both the concurrent year (lag-0) and the year prior to tree growth (lag-1) (Table 2). Statistically significant (95% level or higher) positive correlations were found between WP El Niño and the concurrent rainy season ($\text{Oct}_n\text{-May}_{n+1}$, $r=0.26$). Correlations are strongest with Jan_{n+1} ($r=0.35$), the period of maximum rainy season precipitation. Furthermore, there is a significant correlation with lag-1

January precipitation ($\text{Jan}_n, r=0.22$), indicating a WP El Niño influence on tree growth in the following year. Statistically significant negative correlations were found for La Niña events in January ($\text{Jan}_{n+1}, r=-0.25$) (Table 2). No positive correlation was found between the tree-ring proxy and the CT ENSO index (Table 2). As noted, the CT ENSO flavor has a weaker influence over Java (Fig. 1), therefore we expected the lag-0 correlation to be insignificant. For reference, we also present the correlation with the standard ENSO index NINO3.4, which shows no significance.

Although the $\delta^{18}\text{O}_{\text{TR}}$ record correlates significantly ($p<0.05$) with ENSO flavors, the response is not stationary. Fig. 2 presents the running 31-year correlation and Kalman filter analysis between the varying ENSO flavors and the tree-ring proxy for the period of highest correlation (see Table 2). The teleconnection with Jan_{n+1} WP ENSO is strong and significantly positive from the 1950s until present, with running correlations reaching 0.6, and an r of 0.45 for AD 1950-2007 ($p<0.001$) (Fig. 2a). However, before 1950 the correlation falls to zero, and even becomes negative. The Kalman filter time-varying regression coefficients (beta weights) follow the same trend as the correlation values and reinforce the time dependency of the teleconnection. From 1950 onwards, the lower limits do not cross zero, which means that the beta weights are considered statistically significant. However, the correlation weakens slightly again in the beginning of the 21st century. The relationship with Jan_{n+1} NINO4 (used here to primarily capture La Niña events) (Fig. 2c) is also time dependent with weak correlations before 1950 and after 2000, but a significant negative relationship in the second half of the century with $r=-0.37$ ($p<0.01$).

The fingerprints of the ENSO flavors in the $\delta^{18}\text{O}_{\text{TR}}$ record can be seen in the probability density function (PDF) of $\delta^{18}\text{O}_{\text{TR}}$ anomalies (Fig. 3) conditioned on ENSO phase. The $\delta^{18}\text{O}_{\text{TR}}$ probability mass for WP El Niño is skewed towards positive anomalies associated with dry conditions. By contrast, the PDF for CT El Niño events exhibits bimodality with peaks in both positive and negative $\delta^{18}\text{O}_{\text{TR}}$ anomalies, suggesting this record is not a good proxy for CT El Niño variability.

To further investigate expressions of ENSO variability in the $\delta^{18}\text{O}_{\text{TR}}$ record we performed spectral analysis (Fig. 4a). Spectral analysis of the $\delta^{18}\text{O}_{\text{TR}}$ record reveals a broad peak at 2–4 years, falling within the classic ENSO bandwidth (Sarachik and Cane, 2010) as well as significant, decadal-to-multidecadal variability (12.5 years). Wavelet coherence analysis between the proxy record and the WP ENSO and CT ENSO index (Fig. 4b,c) indicates that the coherence varies in time across most spectral bands. The periods of greatest coherence in

time occur on inter-annual timescales (2-4 years), again spanning the classic ENSO bandwidth. We found no significant coherence with CT ENSO index as expected.

4 Discussion

The positive correlation pattern between the $\delta^{18}\text{O}_{\text{TR}}$ record and the WP ENSO index, as well as the negative correlation with La Niña events, supports the conclusion in Schollaen et al. (2013) that the formation of annual $\delta^{18}\text{O}$ in Javanese teak trees is dominated by precipitation patterns. El Niño events are linked to drought conditions over the IMC coinciding with increased $\delta^{18}\text{O}$ values in the tree-ring proxy (Figs 2, 3). The opposite occurs during La Niña events.

The PDFs illustrate a clear WP El Niño and a less strong La Niña signal, with really dry years linked to WP El Niños. In contrast, no clear CT El Niño signal is preserved in the $\delta^{18}\text{O}_{\text{TR}}$ record, as indicated by the bimodality in the corresponding PDF. The different seasonal rainfall signals (wet and dry season rainfall) in the $\delta^{18}\text{O}_{\text{TR}}$ record are damped in the annually resolved proxy due to seasonally alternating isotope signatures in $\delta^{18}\text{O}$ of precipitation (Schollaen et al., 2013). Thus, CT El Niño signals seem to be obscured when followed by a La Niña event. This is the case for the strong CT El Niño event in 1982/83 that was followed by a La Niña, resulting in a low $\delta^{18}\text{O}_{\text{TR}}$ value (Fig. 2b, 2c). High-resolution intra-annual $\delta^{18}\text{O}_{\text{TR}}$ analyses help to disentangle the contrasting isotope effects of dry and rainy season rainfall patterns, as demonstrated in Schollaen et al. (2014). We conclude that the annually resolved tree-ring proxy is suitable for distinguishing between WP El Niño and La Niña, but not for CT El Niños. Correlation tests (Table 2) with a standard ENSO index (such as NINO3.4) show no correlation with the tree-ring record, as this index captures mixed signals from both ENSO flavors. Overall, the strongest and most significant ENSO signal in the tree-ring proxy data is that of WP El Niño.

Our analysis shows that the teleconnections described above are not stationary (Figs 2, 4). There is a drop in correlation in the first half of the 20th century. One can speculate this weakening teleconnection is related to the pattern of relatively weak and irregular ENSO activity in the middle of the 20th century (Tudhope et al., 2001). Arguably, there may be other factors (e.g. Indian Ocean Dipole Mode) determining wetter or drier conditions in this period and the ENSO phenomenon may play a secondary role. In recent decades, a climate regime transition has preceded periods of strong and sustained ENSO events (e.g. O'Kane et al., 2014), leading to a stronger ENSO fingerprint in the $\delta^{18}\text{O}_{\text{TR}}$ record. Furthermore, Chang et al.

(2004) reveal an interdecadal trend of increasing correlations between Indonesian monsoon rainfall and ENSO beginning in the late 1970s.

The $\delta^{18}\text{O}_{\text{TR}}$ record is a rainfall indicator for wet and dry season rainfall, albeit largely dominated by the wet season signal (Scholleen et al., 2013). Note, that the "amount effect" leads to different isotopic signatures in $\delta^{18}\text{O}_{\text{TR}}$ values during wet and dry season. Thus, the dry season rainfall signal, which tends to have the highest coherence with ENSO, is damped in the annually resolved $\delta^{18}\text{O}_{\text{TR}}$ record by the following wet season signal. This may explain the low correlation between the tree-ring proxy and June to November ENSO indices. To distinguish the causes of inter-annual rainfall variability across Java future work needs to focus on high-resolution $\delta^{18}\text{O}_{\text{TR}}$ records.

5 Conclusions

In this study we used a $\delta^{18}\text{O}_{\text{TR}}$ chronology from teak (*Tectona grandis*) that correlates significantly with regional precipitation over Java (Scholleen et al., 2013) to examine various manifestations of ENSO. This is the first time a high-resolution $\delta^{18}\text{O}_{\text{TR}}$ record is used to detect signals of ENSO flavors in palaeoclimatic data as argued by Karamperidou et al. (2015). These results indicate the potential for generating reconstructions of different ENSO flavors from high-resolution intra-annual $\delta^{18}\text{O}$ records from appropriately selected regions, such as Java. Such palaeoclimatic records may help answer the many remaining questions surrounding the diversity of ENSO activity and past ENSO variability. In addition, the conclusions of our study call for caution when attempting to interpret proxy records using ENSO indices that are not able to distinguish between the two flavors (e.g. single standard indices such as NINO3.4). As shown here, single ENSO indices may capture mixed signals from both flavors, resulting in lower correlations with proxies and thus confounding paleoclimate reconstruction attempts. Furthermore, performing model-proxy comparisons using single ENSO indices may be misleading. For example, in multi-proxy reconstructions where proxies from different regions can be synthesized to reconstruct past ENSO variability it is important to account for the distinct (and often of opposite sign) influence of two flavors: convoluting their signals by using a single ENSO index can lead to potential misinterpretation of significant changes in past ENSO variability, as in the case of mid-Holocene (6ka BP) coral proxies from the central Pacific (Karamperidou et al., 2015).

Last, our study calls for more emphasis on sampling long-term terrestrial $\delta^{18}\text{O}_{\text{TR}}$ records at seasonal and monthly resolution from selected regions such as northern or eastern Indonesia. Such high-resolution terrestrial $\delta^{18}\text{O}_{\text{TR}}$ records may have stronger correlations with ENSO

flavors, and thus be appropriate for robust reconstructions of wet and dry season rainfall and of past variability of the two ENSO flavors.

Acknowledgements

We acknowledge the Bolin Centre's, Climate Research Summer School during which this project and collaboration was conceived. We also thank two anonymous reviewers who provided excellent suggestions that improved the paper. Karina Schollaen was funded by the HIMPAC (HE 3089/4-1) and the CADY (BMBF, 03G0813H) project. Isotope analyses were funded by a Joint DFG/FAPESP Research Grant (HE3089/5-1). Christina Karamperidou is funded by NSF Award 1304910. Lamont-Doherty Earth Observatory contribution number 0000.

References

- Abram, N. J., Gagan, M. K., Cole, J. E., Hantoro, W. S., and Mudelsee, M.: Recent intensification of tropical climate variability in the Indian Ocean, *Nature Geosci*, 1, 849-853, 2008.
- Adler, R. F., Huffman, G. J., Chang, A., Ferraro, R., Xie, P.-P., Janowiak, J., Rudolf, B., Schneider, U., Curtis, S., Bolvin, D., Gruber, A., Susskind, J., Arkin, P., and Nelkin, E.: The Version-2 Global Precipitation Climatology Project (GPCP) Monthly Precipitation Analysis (1979–Present), *Journal of Hydrometeorology*, 4, 1147-1167, 2003.
- Aldrian, E., Dümenil Gates, L., and Widodo, F. H.: Seasonal variability of Indonesian rainfall in ECHAM4 simulations and in the reanalyses: The role of ENSO, *Theoretical and Applied Climatology*, 87, 41-59, 2007.
- Aldrian, E. and Susanto, R. D.: Identification of three dominant rainfall regions within Indonesia and their relationship to sea surface temperature, *International Journal of Climatology*, 23, 1435-1452, 2003.
- Allan, J. R.: ENSO and Climatic Variability in the Past 150 Years. In: *El Niño and the Southern Oscillation: Multiscale Variability and Global and Regional Impacts*, Diaz, H. F. and Markgraf, V. (Eds.), Cambridge University Press, 2000.
- Araguás-Araguás, L., Froehlich, K., and Rozanski, K.: Deuterium and oxygen-18 isotope composition of precipitation and atmospheric moisture, *Hydrological Processes*, 14, 1341-1355, 2000.
- Ashok, K., Behera, S. K., Rao, S. A., Weng, H., and Yamagata, T.: El Niño Modoki and its possible teleconnection, *Journal of Geophysical Research: Oceans*, 112, C11007, 2007.
- Ashok, K. and Yamagata, T.: Climate change: The El Niño with a difference, *Nature*, 461, 481-484, 2009.
- Barbour, M. M.: Stable oxygen isotope composition of plant tissue: a review, *Functional Plant Biology*, 34, 83-94, 2007.
- Braganza, K., Gergis, J. L., Power, S. B., Risbey, J. S., and Fowler, A. M.: A multiproxy index of the El Niño–Southern Oscillation, A.D. 1525–1982, *Journal of Geophysical Research: Atmospheres*, 114, D05106, 2009.
- Brienen, R. J. W., Helle, G., Pons, T. L., Guyot, J. L., and Gloor, M.: Oxygen isotopes in tree rings are a good proxy for Amazon precipitation and El Niño–Southern Oscillation variability, *Proceedings of the National Academy of Sciences*, 109, 16957-16962, 2012.
- Chang, C. P., Wang, Z., Ju, J., and Li, T.: On the Relationship between Western Maritime Continent Monsoon Rainfall and ENSO during Northern Winter, *J. Clim.*, 17, 665-672, 2004.
- Charles, C. D., Cobb, K., Moore, M. D., and Fairbanks, R. G.: Monsoon–tropical ocean interaction in a network of coral records spanning the 20th century, *Marine Geology*, 201, 207-222, 2003.
- Clement, A. C., Seager, R., and Murtugudde, R.: Why Are There Tropical Warm Pools?, *J. Clim.*, 18, 5294-5311, 2005.
- Cobb, K. M., Westphal, N., Sayani, H. R., Watson, J. T., Di Lorenzo, E., Cheng, H., Edwards, R. L., and Charles, C. D.: Highly Variable El Niño–Southern Oscillation Throughout the Holocene, *Science*, 339, 67-70, 2013.
- Collins, M., An, S.-I., Cai, W., Ganachaud, A., Guilyardi, E., Jin, F.-F., Jochum, M., Lengaigne, M., Power, S., Timmermann, A., Vecchi, G., and Wittenberg, A.: The impact of global warming on the tropical Pacific Ocean and El Niño, *Nature Geosci*, 3, 391-397, 2010.
- Cook, E. R., D'Arrigo, R. D., and Mann, M. E.: A Well-Verified, Multiproxy Reconstruction of the Winter North Atlantic Oscillation Index since A.D. 1400*, *J. Clim.*, 15, 1754-1764, 2002.
- Cook, E. R., Palmer, J. G., Ahmed, M., Woodhouse, C. A., Fenwick, P., Zafar, M. U., Wahab, M., and Khan, N.: Five centuries of Upper Indus River flow from tree rings, *Journal of Hydrology*, 486, 365-375, 2013.

1 Coster, C.: Zur Anatomie und Physiologie der Zuwachszonen- und Jahresringbildung in den
2 Tropen, *Ann. Jard. Bot. Buitenzong*, 38, 1-114, 1928.

3 Coster, C.: Zur Anatomie und Physiologie der Zuwachszonen- und Jahresringbildung in den
4 Tropen, *Ann. Jard. Bot. Buitenzong*, 37, 49-160, 1927.

5 D'Arrigo, R., Cook, E. R., Wilson, R. J., Allan, R., and Mann, M. E.: On the variability of
6 ENSO over the past six centuries, *Geophys. Res. Lett.*, 32, L03711, 2005.

7 D'Arrigo, R., Wilson, R., Palmer, J., Krusic, P., Curtis, A., Sakulich, J., Bijaksana, S.,
8 Zulaikah, S., Ngkoimani, L. O., and Tudhope, A.: The reconstructed Indonesian warm pool
9 sea surface temperatures from tree rings and corals: Linkages to Asian monsoon drought and
10 El Niño–Southern Oscillation, *Paleoceanography*, 21, PA3005, 2006.

11 Emile-Geay, J., Cobb, K. M., Mann, M. E., and Wittenberg, A. T.: Estimating Central
12 Equatorial Pacific SST Variability over the Past Millennium. Part II: Reconstructions and
13 Implications, *J. Clim.*, 26, 2329-2352, 2013.

14 Evans, M. N., Kaplan, A., and Cane, M. A.: Pacific sea surface temperature field
15 reconstruction from coral $d^{18}O$ data using reduced space objective analysis,
16 *Paleoceanography*, 17, 7-1-7-13, 2002.

17 Fowler, A. M., Boswijk, G., Lorrey, A. M., Gergis, J., Pirie, M., McCloskey, S. P. J., Palmer,
18 J. G., and Wunder, J.: Multi-centennial tree-ring record of ENSO-related activity in New
19 Zealand, *Nature Clim. Change*, 2, 172-176, 2012.

20 Geiger, F.: Anatomische Untersuchungen über die Jahresringbildung von *Tectona grandis*. In:
21 *Jahrbücher für wissenschaftliche Botanik*, Pfeffer, W. (Ed.), 1915.

22 Grinsted, A., Moore, J. C., and Jevrejeva, S.: Application of the cross wavelet transform and
23 wavelet coherence to geophysical time series, *Nonlin. Processes Geophys.*, 11, 561-566,
24 2004.

25 Haylock, M. and McBride, J.: Spatial Coherence and Predictability of Indonesian Wet Season
26 Rainfall, *J. Clim.*, 14, 3882-3887, 2001.

27 Hendon, H. H.: Indonesian Rainfall Variability: Impacts of ENSO and Local Air-Sea
28 Interaction, *J. Clim.*, 16, 1775-1790, 2003.

29 Jourdain, N., Gupta, A., Taschetto, A., Ummenhofer, C., Moise, A., and Ashok, K.: The Indo-
30 Australian monsoon and its relationship to ENSO and IOD in reanalysis data and the
31 CMIP3/CMIP5 simulations, *Climate Dynamics*, 41, 3073-3102, 2013.

32 Kao, H.-Y. and Yu, J.-Y.: Contrasting Eastern-Pacific and Central-Pacific Types of ENSO, *J.*
33 *Clim.*, 22, 615-632, 2009.

34 Kaplan, A., Cane, M., Kushnir, Y., Clement, A., Blumenthal, M., and Rajagopalan, B.:
35 Analyses of global sea surface temperature 1856–1991, *Journal of Geophysical Research-*
36 *Oceans*, 103, 18567-18589, 1998.

37 Karamperidou, C., Di Nezio, P. N., Timmermann, A., Jin, F.-F., and Cobb, K. M.: The
38 response of ENSO flavors to mid-Holocene climate: Implications for proxy interpretation,
39 *Paleoceanography*, 30, 527-547, 2015.

40 Kug, J.-S. and Ham, Y.-G.: Are there two types of La Nina?, *Geophysical Research Letters*,
41 38, L16704, 2011.

42 Kug, J.-S., Jin, F.-F., and An, S.-I.: Two Types of El Niño Events: Cold Tongue El Niño and
43 Warm Pool El Niño, *J. Clim.*, 22, 1499-1515, 2009.

44 Kumar, K. K., Rajagopalan, B., Hoerling, M., Bates, G., and Cane, M.: Unraveling the
45 Mystery of Indian Monsoon Failure During El Niño, *Science*, 314, 115-119, 2006.

46 Larkin, N. K. and Harrison, D. E.: On the definition of El Niño and associated seasonal
47 average U.S. weather anomalies, *Geophysical Research Letters*, 32, L13705, 2005.

48 Lau, N.-C. and Nath, M. J.: Impact of ENSO on the Variability of the Asian–Australian
49 Monsoons as Simulated in GCM Experiments, *J. Clim.*, 13, 4287-4309, 2000.

50 Lee, T. and McPhaden, M. J.: Increasing intensity of El Niño in the central-equatorial Pacific,
51 *Geophys. Res. Lett.*, 37, L14603, 2010.

1 Linsley, B. K., Wellington, G. M., Schrag, D. P., Ren, L., Salinger, M. J., and Tudhope, A.
2 W.: Geochemical evidence from corals for changes in the amplitude and spatial pattern of
3 South Pacific interdecadal climate variability over the last 300 years, *Climate Dynamics*, 22,
4 1-11, 2004.

5 Mann, M. E., Gille, E., Overpeck, J., Gross, W., Bradley, R. S., Keimig, F. T., and Hughes,
6 M. K.: Global Temperature Patterns in Past Centuries: An Interactive Presentation, *Earth*
7 *Interactions*, 4, 1-1, 2000.

8 McCarroll, D. and Loader, N. J.: Stable isotopes in tree rings, *Quaternary Science Reviews*,
9 23, 771-801, 2004.

10 McPhaden, M. J., Lee, T., and McClurg, D.: El Niño and its relationship to changing
11 background conditions in the tropical Pacific Ocean, *Geophysical Research Letters*, 38,
12 L15709, 2011.

13 Newman, M., Shin, S.-I., and Alexander, M. A.: Natural variation in ENSO flavors,
14 *Geophysical Research Letters*, 38, L14705, 2011.

15 O'Kane, T. J., Matear, R. J., Chamberlain, M. A., and Oke, P. R.: ENSO regimes and the late
16 1970's climate shift: The role of synoptic weather and South Pacific ocean spiciness, *Journal*
17 *of Computational Physics*, 271, 19-38, 2014.

18 Pfeiffer, M., Dullo, W.-C., Zinke, J., and Garbe-Schönberg, D.: Three monthly coral Sr/Ca
19 records from the Chagos Archipelago covering the period of 1950–1995 A.D.: reproducibility
20 and implications for quantitative reconstructions of sea surface temperature variations,
21 *International Journal of Earth Sciences*, 98, 53-66, 2009.

22 Pierrehumbert, R. T.: Thermostats, Radiator Fins, and the Local Runaway Greenhouse,
23 *Journal of the Atmospheric Sciences*, 52, 1784-1806, 1995.

24 Quinn, T. M., Taylor, F. W., and Crowley, T. J.: Coral-based climate variability in the
25 Western Pacific Warm Pool since 1867, *Journal of Geophysical Research: Oceans*, 111,
26 C11006, 2006.

27 Ren, H.-L. and Jin, F.-F.: Niño indices for two types of ENSO, *Geophysical Research Letters*,
28 38, L04704, 2011.

29 Sano, M., Xu, C., and Nakatsuka, T.: A 300-year Vietnam hydroclimate and ENSO variability
30 record reconstructed from tree ring $\delta^{18}\text{O}$, *Journal of Geophysical Research*, 117, D12115,
31 2012.

32 Sarachik, E. S. and Cane, M. A.: *The El Niño-Southern Oscillation Phenomenon*, Cambridge
33 University Press, London, 2010.

34 Schollaen, K., Heinrich, I., and Helle, G.: UV-laser-based microscopic dissection of tree rings
35 – a novel sampling tool for $\delta^{13}\text{C}$ and $\delta^{18}\text{O}$ studies, *New Phytologist*, 201, 1045-1055, 2014.

36 Schollaen, K., Heinrich, I., Neuwirth, B., Krusic, P. J., D'Arrigo, R. D., Karyanto, O., and
37 Helle, G.: Multiple tree-ring chronologies (ring width, $\delta^{13}\text{C}$ and $\delta^{18}\text{O}$) reveal dry and rainy
38 season signals of rainfall in Indonesia, *Quaternary Science Reviews*, 73, 170-181, 2013.

39 Schulman, E.: *Dendroclimatic Change in Semiarid America*, University of Arizona Press,
40 Tuscon, Arizona, 1956.

41 Schulz, M. and Mudelsee, M.: REDFIT: estimating red-noise spectra directly from unevenly
42 spaced paleoclimatic time series, *Computers & Geosciences*, 28, 421-426, 2002.

43 Stahle, D. W., Cleaveland, M. K., Therrell, M. D., Gay, D. A., D'Arrigo, R. D., Krusic, P. J.,
44 Cook, E. R., Allan, R. J., Cole, J. E., Dunbar, R. B., Moore, M. D., Stokes, M. A., Burns, B.
45 T., Villanueva-Diaz, J., and Thompson, L. G.: Experimental Dendroclimatic Reconstruction
46 of the Southern Oscillation, *Bulletin of the American Meteorological Society*, 79, 2137–2152,
47 1998.

48 Takahashi, K., Montecinos, A., Goubanova, K., and Dewitte, B.: ENSO regimes:
49 Reinterpreting the canonical and Modoki El Niño, *Geophysical Research Letters*, 38, L10704,
50 2011.

51 Taschetto, A. S. and England, M. H.: El Niño Modoki impacts on Australian rainfall, *J. Clim.*,
52 22, 3167-3174, 2009.

- 1 Torrence, C. and Compo, G. P.: A Practical Guide to Wavelet Analysis, Bulletin of the
- 2 American Meteorological Society, 79, 61-78, 1998.
- 3 Tudhope, A. W., Chilcott, C. P., McCulloch, M. T., Cook, E. R., Chappell, J., Ellam, R. M.,
- 4 Lea, D. W., Lough, J. M., and Shimmield, G. B.: Variability in the El Niño - Southern
- 5 oscillation through a glacial-interglacial cycle, Science, 291, 1511-1517, 2001.
- 6 Visser, H. and Molenaar, J.: Kalman Filter Analysis in Dendroclimatology, Biometrics, 44,
- 7 929-940, 1988.
- 8 Wheeler, M. C. and McBride, J. L.: Australian-Indonesian monsoon. In: Intraseasonal
- 9 Variability in the Atmosphere-Ocean Climate System, Springer Praxis Books, Springer Berlin
- 10 Heidelberg, 2005.
- 11 Wilson, R., Cook, E., D'Arrigo, R., Riedwyl, N., Evans, M. N., Tudhope, A., and Allan, R.:
12 Reconstructing ENSO: the influence of method, proxy data, climate forcing and
13 teleconnections, Journal of Quaternary Science, 25, 62-78, 2010.
- 14 Wilson, R., Miles, D., Loader, N., Melvin, T., Cunningham, L., Cooper, R., and Briffa, K.: A
15 millennial long March–July precipitation reconstruction for southern-central England,
16 Climate Dynamics, 40, 997-1017, 2013.
- 17 Wilson, R., Tudhope, A., Brohan, P., Briffa, K., Osborn, T., and Tett, S.: Two-hundred-fifty
18 years of reconstructed and modeled tropical temperatures, Journal of Geophysical Research:
19 Oceans, 111, C10007, 2006.
- 20 Yeh, S.-W., Kug, J.-S., Dewitte, B., Kwon, M.-H., Kirtman, B. P., and Jin, F.-F.: El Niño in a
21 changing climate, Nature, 461, 511-514, 2009.
- 22 Zhu, M., Stott, L., Buckley, B., Yoshimura, K., and Ra, K.: Indo-Pacific Warm Pool
23 convection and ENSO since 1867 derived from Cambodian pine tree cellulose oxygen
24 isotopes, Journal of Geophysical Research, 117, D11307, 2012.
- 25

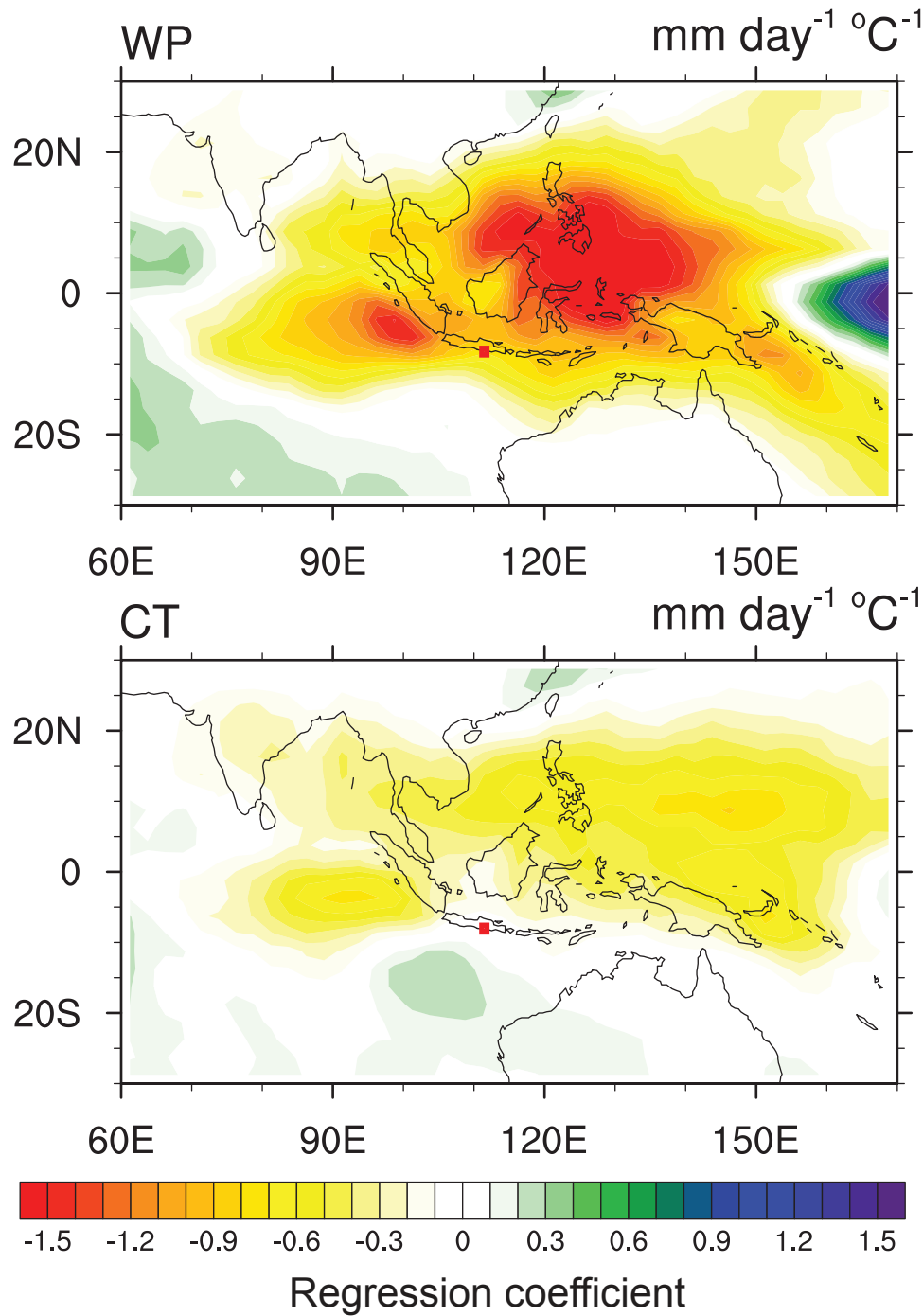
1 Table 1. Classification into ENSO flavors and phase based on Jan_{n+1} values (see section 2.2).
2 Note the use of the southern hemisphere convention (Schulman, 1956), i.e. year n refers to
3 Jan_{n+1} .

ENSO classification	Years										
WP	1900	1902	1904	1907	1913	1927	1929	1939	1941	1957	1958
	1968	1978	1979	1987	1990	1994	2001	2002	2003	2004	
CT	1905	1911	1914	1918	1919	1923	1925	1930	1940	1965	1972
	1976	1982	1986	1991	1997						
LN	1909	1916	1917	1920	1924	1933	1938	1942	1949	1955	1970
	1973	1975	1983	1988	1998	1999	2000	2005	2007		

4

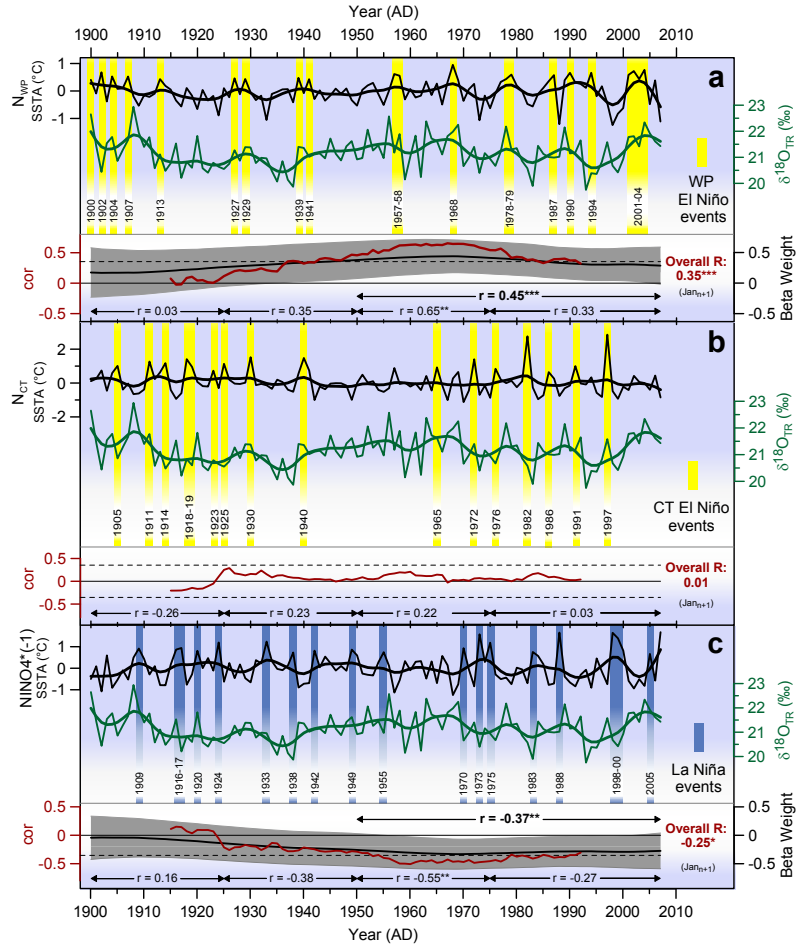
Table 2. Correlation values between the annually resolved $\delta^{18}\text{O}_{\text{TR}}$ record and climate months of different ENSO flavors and the standard NINO3.4 and La Niña index (NINO4*(-1)) for the period from the year prior to growth (lag-1) to the current year (lag-0) and seasonal means (calculated over the 1900-2007 period). (**: $p < 0.001$, *: $p < 0.01$, bold: $p < 0.05$).

Climate months <i>lag1 lag0</i>		WP El Niño	CT El Niño	NINO3.4	La Niña
Oct _{n-1}	Oct _n	0.12 0.21	-0.18 -0.03	-0.10 0.08	0.00 -0.14
Nov _{n-1}	Nov _n	0.17 0.17	-0.23 -0.01	-0.13 0.05	0.00 -0.12
Dec _{n-1}	Dec _n	0.18 0.18	-0.20 0.04	-0.11 0.10	-0.01 -0.15
Jan _n	Jan _{n+1}	0.22 0.35**	-0.19 -0.01	-0.07 0.12	-0.06 -0.25*
Feb _n	Feb _{n+1}	0.15 0.29*	-0.15 -0.06	-0.07 0.09	-0.05 -0.21
Mar _n	Mar _{n+1}	0.05 0.21	-0.17 -0.12	-0.10 0.02	0.03 -0.12
Apr _n	Apr _{n+1}	0.14 0.21	-0.21 -0.09	-0.12 0.01	-0.02 -0.15
May _n	May _{n+1}	0.12 0.20	-0.14 -0.11	-0.06 -0.01	-0.03 -0.12
Jun _n	Jun _{n+1}	0.14 0.08	-0.07 -0.06	0.00 -0.03	-0.08 -0.03
Jul _n	Jul _{n+1}	0.12 0.16	-0.02 -0.08	0.05 -0.03	-0.09 -0.10
Aug _n	Aug _{n+1}	0.11 0.10	-0.02 -0.07	0.07 -0.03	-0.10 -0.05
Sep _n	Sep _{n+1}	0.17 0.01	-0.05 -0.05	0.03 -0.06	-0.11 0.02
peak wet season (Jan _{n+1})		0.35**			-0.25*
Dec _n -Feb _{n+1}		0.27*			-0.21
wet season (Oct _n -May _{n+1})		0.26*			



1

2 Figure 1. Regression coefficients ($\text{mm day}^{-1} \text{ }^{\circ}\text{C}^{-1}$) of monthly precipitation on the Warm Pool
 3 (WP) and the Cold Tongue (CT) ENSO index. The two indices are computed as per Ren and
 4 Jin (2011) (1). Precipitation data are from the GPCP (Adler et al., 2003), for the period 1987-
 5 2010. The tree-ring site is marked with a red square.



1

2 Figure 2. Time series of the $\delta^{18}\text{O}_{\text{TR}}$ chronology (green) and the January (Jan_{n+1}) indices of (a)

3 Warm Pool ENSO (N_{WP}), (b) Cold Tongue ENSO (N_{CT}), and (c) negative NINO4 index

4 ($\text{NINO4}*(-1)$), used here as a La Niña index. The WP and CT ENSO indices are computed as

5 per Ren and Jin (2011) (1). Thick lines denote 10-year cubic smoothing spline. In the lower

6 part of each figure the running 31-year correlation (red) is shown. Dashed horizontal line

7 indicates the 95% confidence level. Also shown are the results from a Kalman filter analysis

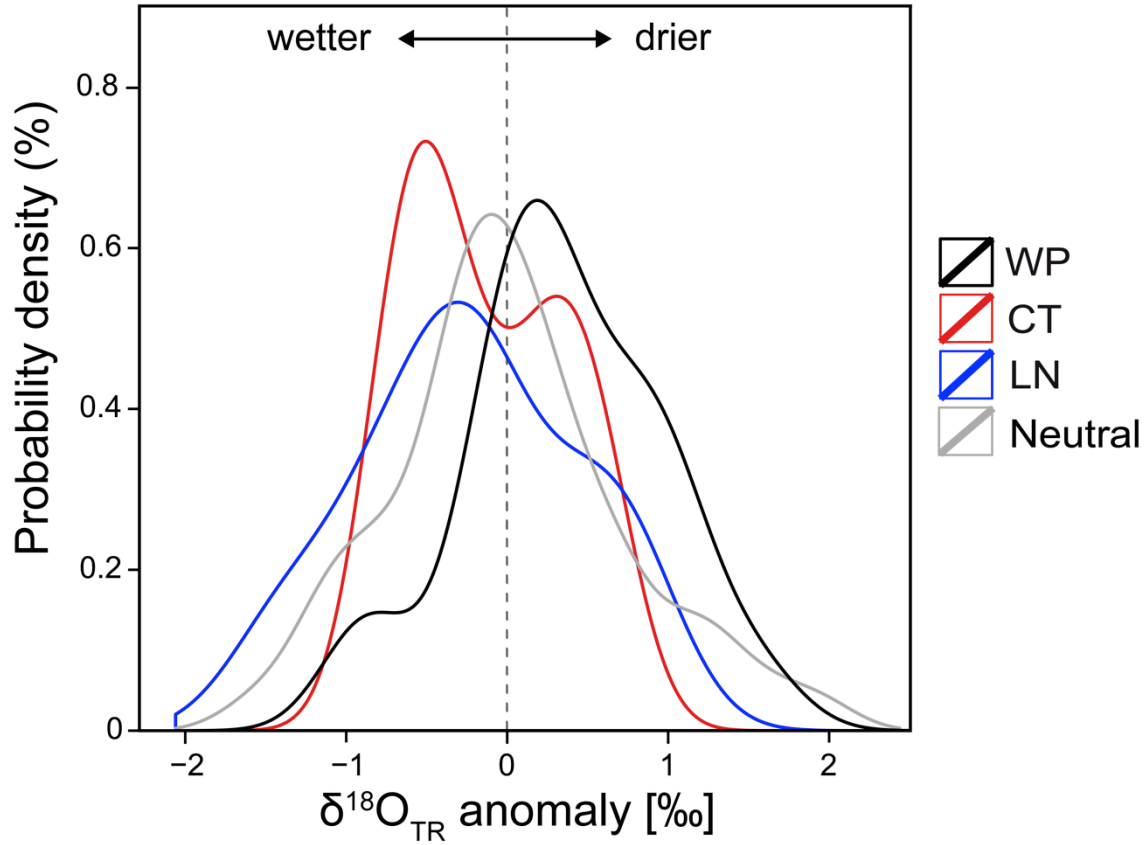
8 (black line) used as a dynamic regression-modeling tool. Grey shading denotes ± 2 standard

9 error limits of the beta weights. Where the limits do not cross zero, the regression relationship

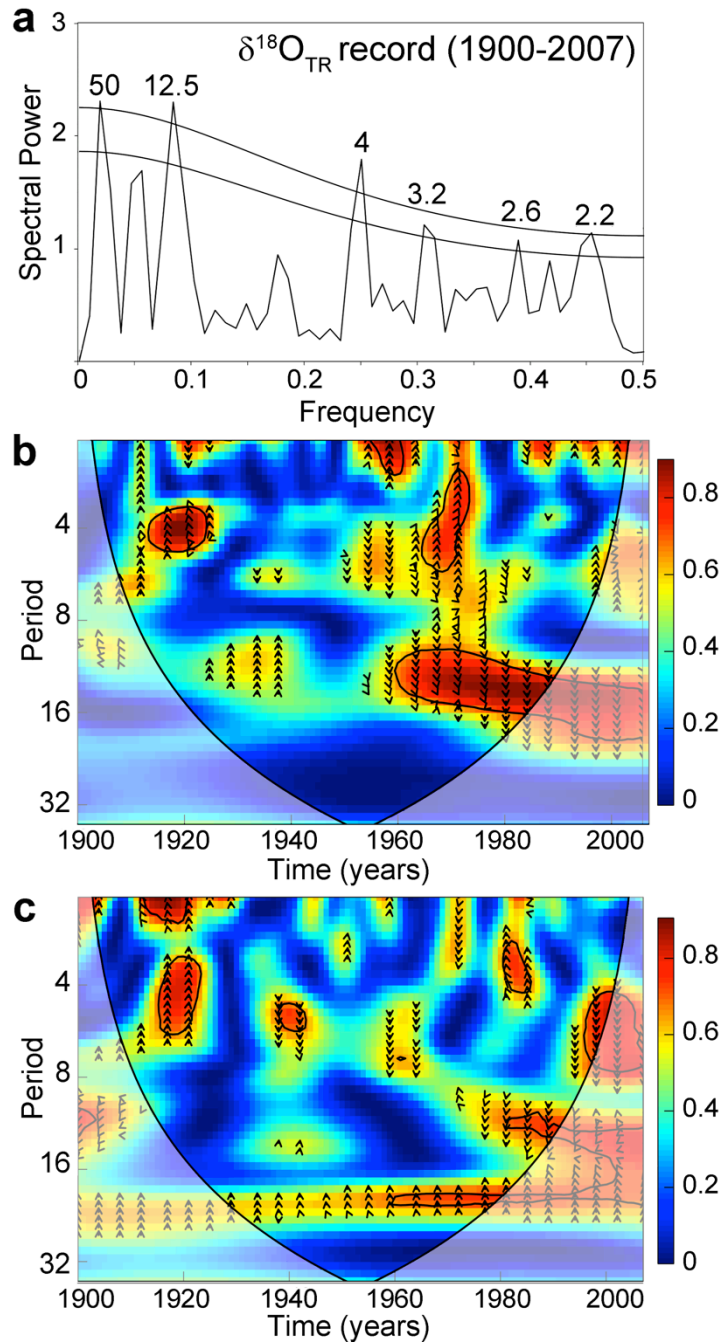
10 are considered statistically significant ($p=95\%$). ENSO events based on classification of Table

11 1 are highlighted in yellow (El Niño) and blue (La Niña), respectively. (** $p < 0.001$, ** $p <$

12 0.01 , * $p < 0.05$).



1
2 Figure 3. Probability density function of tree-ring $\delta^{18}\text{O}$ variability conditional on different
3 ENSO phases: Warm Pool El Niño (WP, black line), Cold Tongue El Niño (CT, red line), La
4 Niña (LN, blue line) and neutral conditions (grey line). For the construction of the PDF, we
5 use January-February ($\text{Jan}_{n+1}\text{Feb}_{n+1}$) time-averaged values; the events considered for each
6 conditional PDF are shown in Table 1.



1

2 Figure 4. (a) Spectral analysis (Schulz and Mudelsee, 2002) of the $\delta^{18}\text{O}_{\text{TR}}$ chronology from
3 1900 to 2007. 90% and 95% confidence levels are indicated. (b) Wavelet coherence transform
4 comparing shared variance as a function of frequency between $\delta^{18}\text{O}_{\text{TR}}$ record and Warm Pool
5 (WP) ENSO index (Jan_{n+1}) and (c) Cold Tongue (CT) ENSO index (Jan_{n+1}) for 1900 to 2007.
6 The wavelet coherence illustrating temporal frequency coherence between the time series at
7 given periods. The thick black contour designates where time series share significant
8 coherence (p=95%) and the cone of influence where edge effects might distort the picture is
9 shown as a lighter shade. Arrows indicate the phase relationship between series with in-phase
10 pointing right and antiphase pointing left.